

# A GAN-Like Approach for Physics-Based Imitation Learning and Interactive Control

PEI XU and IOANNIS KARAMOUZAS, Clemson University, USA



Fig. 1. A physically simulated character performs diverse punch and kick actions responding to the user's input. Our approach provides a flexible way for real-time interactive control without explicit motion tracking.

We present a simple and intuitive approach for interactive control of physically simulated characters. Our work builds upon generative adversarial networks (GAN) and reinforcement learning, and introduces an imitation learning framework where an ensemble of classifiers and an imitation policy are trained in tandem given pre-processed reference clips. The classifiers are trained to discriminate the reference motion from the motion generated by the imitation policy, while the policy is rewarded for fooling the discriminators. Using our GAN-like approach, multiple motor control policies can be trained separately to imitate different behaviors. In runtime, our system can respond to external control signal provided by the user and interactively switch between different policies. Compared to existing method, our proposed approach has the following attractive properties: 1) achieves state-of-the-art imitation performance without manually designing and fine tuning a reward function; 2) directly controls the character without having to track any target reference pose explicitly or implicitly through a phase state; and 3) supports interactive policy switching without requiring any motion generation or motion matching mechanism. We highlight the applicability of our approach in a range of imitation and interactive control tasks, while also demonstrating its ability to withstand external perturbations as well as to recover balance. Overall, our approach has low runtime cost and can be easily integrated into interactive applications and games.

CCS Concepts: • **Computing methodologies** → **Animation; Physical simulation; Reinforcement learning.**

Additional Key Words and Phrases: character animation, physics-based control, reinforcement learning, GAN

## ACM Reference Format:

Pei Xu and Ioannis Karamouzas. 2021. A GAN-Like Approach for Physics-Based Imitation Learning and Interactive Control. *Proc. ACM Comput. Graph. Interact. Tech.* 4, 3 (September 2021), 24 pages. <https://doi.org/10.1145/3480148>

## 1 INTRODUCTION

Data-driven methods have long been used to generate realistic character animation. Kinematic approaches typically rely on a pre-collected reference dataset containing diverse motion clips that are used for motion generation or synthesis without fully leveraging the physical equations of

---

Authors' address: Pei Xu, peix@clemson.edu; Ioannis Karamouzas, ioannis@clemson.edu, School of Computing, Clemson University, USA.

---

© 2021 Copyright held by the owner/author(s). Publication rights licensed to ACM.

This is the author's version of the work. It is posted here for your personal use. Not for redistribution. The definitive Version of Record was published in *Proceedings of the ACM on Computer Graphics and Interactive Techniques*, <https://doi.org/10.1145/3480148>.

motion [Holden et al. 2020, 2017]. Though high-quality animations can be generated depending on the amount and quality of the motion dataset [Clavet 2016], kinematics-based methods may suffer problems when facing complex, unpredicted perturbations or environmental variations. Physics-based methods, on the other hand, perform simulation through a physics engine to generate motions, and thus guarantee the physical realism of the generated motions [Wu and Zordan 2010; Wu and Popović 2010]. Such methods can also enable sim-to-real transfer and apply motion generation techniques on physical robots as shown in recent works [Hwangbo et al. 2019; Peng et al. 2020].

A challenge in physics-based methods for realistic motion generation is that a controller is needed to be optimized either directly by applying joint torques or indirectly through, for example, proportional-derivative (PD) servos to help the character reach a desired pose. However, those control signals are typically inaccessible when we capture motion in the real world. In recent years, reinforcement learning has been widely used to perform the optimization in order to obtain a general controller without pre-assumed heuristic rules. Data-driven methods for imitation learning under the framework of deep reinforcement learning have achieved state-of-the-art performance and are able to generate high-quality motions [Chentanez et al. 2018; Peng et al. 2018; Won et al. 2020]. However, when facing an interactive control demand, methods that rely on motion tracking usually need a motion generation or matching mechanism to ensure the transition between two different behaviors or motor control policies [Bergamin et al. 2019; Won et al. 2020].

In this paper, we propose an alternative approach for motion capture imitation and interactive control of physically simulated characters based on the framework of generative adversarial imitation learning (GAIL) [Ho and Ermon 2016; Merel et al. 2017]. We propose a number of improvements upon GAIL to stabilize the training process, and achieve imitation performance comparable to state-of-the-art methods for motion tracking without the need of designing and fine-tuning a reward function. Using our GAN-like approach, multiple motor control policies are trained separately to imitate different reference motion clips. During runtime, the character can exhibit diverse behaviors through interactive policy switching. Our system can run in real time, as checking the feasibility of switching to a target policy is done by simply performing a forward pass on the discriminators of the target policy. In addition, the policies perform inference using only the last few poses of the character’s trajectory without having to track any target pose. This reduces the system complexity and runtime cost, because no motion generation or matching mechanism is needed for policy transitions. Even though such a solution requires the reference motions to have some similar poses such that the policy switch can happen, it provides a fast and lightweight alternative to the problem of real-time character control. We demonstrate the applicability of our approach in a range of imitation and interactive control tasks, while also highlighting the robustness of the trained controllers to external perturbations.

## 2 BACKGROUND AND RELATED WORK

### 2.1 Physics-Based Character Control

Over the past twenty years, various methods have been proposed for physics-based character control in the fields of computer graphics, robotics and control, including trajectory optimization schemes and reinforcement learning solutions. In the related literature on trajectory optimization methods, a number of controllers have been proposed that focus on specific tasks through manually designed heuristics or feedback rules [Brown et al. 2013; Coros et al. 2010; Lee et al. 2010; Yin et al. 2007]. Online and offline optimization approaches, including model predictive control [Da Silva et al. 2008; Tassa et al. 2012, 2014], open-loop control [Liu et al. 2015, 2010; Mordatch et al. 2012], closed-loop feedback control [da Silva et al. 2017; Liu et al. 2016; Mordatch and Todorov 2014] and model-based control [Hämäläinen et al. 2015; Kwon and Hodgins 2010, 2017], have also been successfully applied

on physics-based character control for motion generation. We refer to the survey from [Geijtenbeek et al. \[2012\]](#) for a general introduction to a variety of optimization approaches for physics-based character control. While characters in most aforementioned works are actuated by joint torques directly or through PD controllers, there are also some interesting works [[Geijtenbeek et al. 2013](#); [Lee et al. 2019, 2014](#); [Nakada et al. 2018](#)] showing the success in muscle-actuated character control.

Approaches based on deep reinforcement learning have gained a lot of popularity recently, allowing to train control policies for simulated characters from raw observation data through trial and error. Goal-conditioned policies that seek to control the character to complete a goal in a physically simulated environment, typically without too much concern about the behavior style, have been employed as baselines in many reinforcement learning test suites and recent algorithms [[Heess et al. 2017](#); [Lillicrap et al. 2015](#); [Schulman et al. 2015a,b, 2017](#)]. However, due to the lack of motion style constraint, the generated motions in these works lack the grace and sophistication exhibited by complex beings. To generate natural motions, many works [[Won et al. 2018](#); [Xie et al. 2020](#); [Yu et al. 2018](#)] use carefully designed reward functions or training strategies to encourage the character to act in an expected style.

To obtain realistic motion, lots of recent works on deep reinforcement learning follow a data-driven approach and achieve state-of-the-art performance through learning to imitate reference examples of expert motion. DeepLoco [[Peng et al. 2017](#)] uses a hierarchical strategy to implement walking style imitation for physics-based humanoid character in navigation tasks. DeepMimic [[Peng et al. 2018](#)] enables a physics-based character to exhibit various motion skills learned from artist-authored animation and motion capture data by combining imitation learning with goal-conditioned learning. [Chentanez et al. \[2018\]](#) builds upon DeepMimic to train a single imitation policy from a large collection of clips and a recovery policy that can be used when the character deviates significantly from the reference motion. [Park et al. \[2019\]](#) leverage the kinematic aspects of unorganized motion data to generate reference motions for the character to imitate. DReCon [[Bergamin et al. 2019](#)] performs imitation learning with the target pose selected from reference motion dataset dynamically according to the desired movement speed, direction and motion style. MotionVAE [[Ling et al. 2020](#)] employs data-driven generative models using variational autoencoders to generate target motion poses for character control. ScaDriver [[Won et al. 2020](#)] proposes a method of learning a policy for diverse behavior control from clustered motion data.

Most imitation learning works mentioned above rely on motion tracking to perform imitation. Typically, such methods employ a motion phase state variable [[Peng et al. 2018, 2017](#)], the target pose at next frames [[Park et al. 2019](#)], or the difference between the character’s current pose and the target pose [[Bergamin et al. 2019](#); [Won et al. 2020](#)] as a part of the input to the policy network for inference. In addition, a carefully designed reward function plays a key role for imitation learning in these works. In this paper, we explore an approach based on generative adversarial networks (GAN) [[Goodfellow et al. 2014](#)] to perform imitation learning through causal inference based on the character’s last pose trajectory only and without any manually designed reward function. Concurrent with our work, [Peng et al. \[2021\]](#) proposed a GAN-like approach to synthesize high-quality motion from large datasets of unstructured motion clips combined with goal-conditioned learning. While their work focuses on goal-directed motion synthesis, our approach focuses on interactively controlling physically simulated characters.

## 2.2 Generative Adversarial Imitation Learning

Generative adversarial imitation learning (GAIL) [[Ho and Ermon 2016](#)] borrows the idea of vanilla generative adversarial networks (GAN) [[Goodfellow et al. 2014](#)] to perform imitation learning. The vanilla GAN optimizes a generative model to produce real-like data by playing a min-max game with a discriminator trained together with the generator. Combining the idea of GAN with

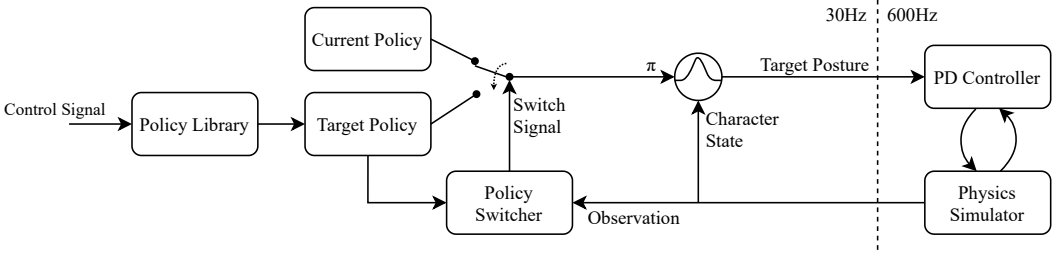


Fig. 2. Overview of our system during runtime. The policy switcher uses the character’s observation to decide whether to keep the currently activated policy or to switch to the target policy interactively responding to the external control signal when such a transition is considered feasible. The activated policy network queries the character state from the physics simulator and outputs target angles to the PD controller. Joint torques are computed from PD servos and applied to the character model.

reinforcement learning, GAIL utilizes a discriminator to identify the agent’s actions from the expert ones, and generates reward signal for reinforcement learning when the agent is able to fool the discriminator. GAIL, based on the vanilla GAN, trains the discriminator as a binary classifier to minimize the cross-entropy loss:

$$- E_{(s_t, a_t)} [\log D(s_t, a_t)] - E_{(\tilde{s}_t, \tilde{a}_t)} [\log(1 - D(\tilde{s}_t, \tilde{a}_t))], \quad (1)$$

where  $(s_t, a_t)$  is the state-action pair taken by the agent under training at the time step  $t$  and  $(\tilde{s}_t, \tilde{a}_t)$  is that taken by the expert. The work from Merel et al. [2017] extends GAIL and proposes to use  $(s_t, s_{t+1})$  as a substitute of  $(s_t, a_t)$  in the case where the expert action is inaccessible.

GAIL provides a way of imitation learning without interacting with the expert during training. This is similar to inverse reinforcement learning (IRL) [Ng et al. 2000; Russell 1998] methods, though IRL explicitly recovers a reward function from expert data before policy extraction. Through the extension to GAIL proposed by Merel et al. [2017], we can perform imitation learning from motion capture data directly for character control by pose comparison without accessing the control signals. Despite such recent advancements, GAIL-based methods can be quite unstable because of the difficulty to find the Nash equilibrium between the generator (policy network) and discriminator, resulting in subpar imitation performance.

Our approach of imitation learning for physically simulated characters builds off of the GAIL framework from Merel et al. [2017]. To improve the stability of adversarial training, though, we propose a number of improvements as detailed in Section 4. Our approach exhibits comparable performance with the state-of-the-art imitation learning methods, and provides a novel way to perform interactive control for physics-based characters.

### 3 OVERVIEW

Our system implements interactive control of physically simulated characters by supporting a range of behaviors through imitation learning and policy switching. In a pre-processing phase, we first collect a number of motion clips that cover specific behaviors. We use these clips to synthesize reference motions that we want the character to imitate (see Section 6 for details), and create a library of physics-based controllers by training corresponding action policies (Section 5). All policies are trained using a GAN-like approach under the GAIL framework (Section 4). As such, we do not have to manually design a reward function for imitation learning. We make several improvements over the vanilla GAIL framework and ensure that our GAN-like approach can provide comparable performance to the state-of-the-art imitation learning algorithms for physics-based characters.

During runtime, the user can select a target behavior to be performed by the character via any input device. The system responds to the user's control signal and attempts to switch the current policy to the target one, which enables the character to perform a specific action by providing a target posture to angular PD servos. Policies trained with our approach imitate given reference motions and perform inference based only on the short-term pose trajectory of the character. Therefore, they can directly take over the character when given a pose trajectory similar to that in the reference motions, without having to track any target reference pose. We exploit the discriminators trained with the target policy as a *policy switcher* to measure the similarity of the current pose trajectory of the character to the reference motions, and decide if the transition to the target policy is feasible. Figure 2 shows a schematic overview of our system during runtime.

#### 4 GAN-LIKE APPROACH FOR IMITATION LEARNING

The vanilla GAIL framework [Ho and Ermon 2016] performs reinforcement learning by generating reward signals through a discriminator, which outputs a probabilistic result denoting the likelihood of a given state-action sample to be drawn from the expert policy. However, this method cannot be directly applied to the problem of imitation learning from motion clips, as, in general, we cannot directly access the actions (joint torques or target postures to PD servos). As such, we follow the strategy from Merel et al. [2017] and use transitions of the character's observations as the input to the discriminator.

A typical problem of using a GAN-like approach for reinforcement learning is reward signal vanishing. In such a case, the discriminator is too harsh and always gives a very low reward to the agent under training regardless of what progress the agent makes, which result in the training being unable to carry on. This issue is actually similar to the problem of gradient vanishing in vanilla GAN applications, often caused by over-optimization of the discriminator. An exactly opposite situation occurs when the discriminator is under-optimized and unable to effectively identify observation samples from the agent under training. As a result, the agents under such a situation would be "self-satisfied" and cannot be improved to learn to imitate the reference motion accurately. To solve these problems and improve the stability and performance for imitation learning from motion clips through a GAN-like approach, we adopt three tricks: 1) leveraging multiple discriminators as an ensemble; 2) using hinge loss for discriminator training instead of the binary cross entropy loss employed by GAIL; and 3) introducing a gradient penalty term [Gulrajani et al. 2017] during discriminator optimization. We refer to Fig. 3 for a schematic overview of the training process of our proposed GAN-like approach.

##### 4.1 Observation Space

We use the local position and orientation (measured in the unit of quaternion) of the character links relative to the root position and heading direction as the observation space of the discriminator. To embed the movement of the character in the simulated world, we take into account the observations from five consecutive frames relative to the root position and heading direction in the last frame.

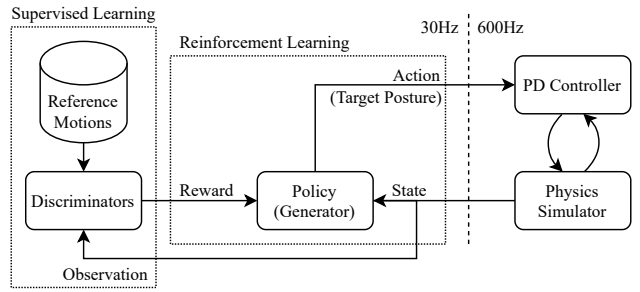


Fig. 3. Schematic overview of training a physics-based character controller from reference motion using our GAN-like approach with reinforcement learning.

Given the observation  $\mathbf{o}_{t-3:t+1} \in \mathbb{R}^{5 \times 7 \times |\mathcal{B}|}$  where  $\mathcal{B}$  is the collection of the character body links, the  $i$ -th discriminator,  $D_i(\mathbf{o}_{t-3:t+1})$ , is trained to identify if the pose trajectory represented by  $\mathbf{o}_{t-3:t+1}$  is from the reference motion or is taken by the agent under training. This provides the appropriate reward signal at time step  $t$  for policy training using reinforcement learning.

## 4.2 Multiple Discriminators

An ignorant agent trained from scratch typically needs to do a large amount of exploration early on during training before reaching some poses similar to those in the reference motion. In contrast, an effective discriminator could easily identify samples from the character agent at the early phases of training and generate low reward signals, which do not encourage the agent's exploration. To address this issue, We employ an ensemble discriminator using the average score from multiple discriminators. Ensemble is a common machine learning technique to produce better predictive model based on multiple base models [Dietterich 2000]. Work from Durugkar et al. [2016] explores the feasibility of using GAN with an ensemble discriminator in image generation tasks.

In our implementation, multiple discriminators are initialized randomly but share the same feature extraction layers. Such an architecture can help avoid model collapse caused by overfitting of single discriminator. It could also prevent reward signal vanishing at the early stages of training by increasing the difficulty of optimization caused by the discrepancy of multiple discriminators. In Section 6, we empirically show the effect that different number of discriminators have on the performance.

## 4.3 Hinge-Loss Optimization

To avoid over-optimization of the discriminator, we use a hinge version of the discriminator loss (Eq. 1) as proposed by Lim and Ye [2017]:

$$\mathcal{L}_{D_i} = \mathbb{E} [\max(0, 1 + D_i(\mathbf{o}_{t-3:t+1}))] + \mathbb{E} [\max(0, 1 - D_i(\tilde{\mathbf{o}}_{t-3:t+1}))], \quad (2)$$

where  $\mathbf{o}_{t-3:t+1}$  are observation samples from the character agent and  $\tilde{\mathbf{o}}_{t-3:t+1}$  are samples drawn from reference motion clips that the character agent intends to imitate. This loss function borrows the idea of support vector machine optimization with soft margin. Minimizing Eq. 2 is equivalent to optimizing the discriminator to perform classification based on the separating hyperplane of 0 with margin of 1. This loss function prevents over-optimization by avoiding performing optimization over samples that have been classified correctly, i.e. samples satisfying  $D_i(\mathbf{o}_{t-3:t+1}) \leq -1$  or  $D_i(\tilde{\mathbf{o}}_{t-3:t+1}) \geq 1$ . GAN with hinge loss has been adopted by many works in the field of image generation [Brock et al. 2018; Miyato et al. 2018; Zhang et al. 2019].

When switching to a hinge loss, the discriminators do not provide anymore a probabilistic result, but a score, with a valid range of  $[-1, 1]$ , expressed as a *monotonic* measurement of the similarity between a given pose trajectory and segments in the reference motion. This property is important, as we can use this score as a reward signal that has a clearly defined upper and lower bound, and monotonically increases with the similarity of the given pose trajectory and the reference motion.

## 4.4 Gradient Penalty

The gradient penalty term was introduced by WGAN-GP [Gulrajani et al. 2017] as a regularization term added to discriminator loss function to enforce the 1-Lipschitz constraint, thereby preventing gradient explosion and vanishing, and improving the stability of training. The gradient penalty term for the  $i$ -th discriminator in our implementation is computed as

$$\mathcal{L}_{D_i}^{GP} = \mathbb{E} [(||\nabla_{\tilde{\mathbf{o}}_{t-3:t+1}} D_i(\tilde{\mathbf{o}}_{t-3:t+1})||_2 - 1)^2], \quad (3)$$

where  $\hat{\mathbf{o}}_{t-3:t+1} = \alpha \tilde{\mathbf{o}}_{t-3:t+1} + (1 - \alpha) \mathbf{o}_{t-3:t+1}$  with the interpolation coefficient  $\alpha$  drawn uniformly between 0 and 1 for each training sample pair  $(\tilde{\mathbf{o}}_{t-3:t+1}, \mathbf{o}_{t-3:t+1})$ .  $\hat{\mathbf{o}}_{t-3:t+1}$  denotes the interpolation of samples between the reference motion and the ones from the agent under training, and is exploited to emulate all possible samples distributed along the manifold of the valid observation space. This regularization term actually intends to optimize the discriminator network such that the gradient norm with respect to all possible observations is close to 1.

Overall, our ensemble with  $N$  discriminators approach has the following loss function:

$$\mathcal{L}_D = \frac{1}{N} \sum_{i=1}^N \left( \mathcal{L}_{D_i} + \lambda^{GP} \mathcal{L}_{D_i}^{GP} \right), \quad (4)$$

where  $\lambda^{GP}$  is a scalar coefficient. In our implementation, all discriminators share the same layers before the final one, as shown in Fig. 4. The final layer linked to each discriminator is initialized independently and randomly to provide diversity. Our approach of discriminator ensemble is different than average pooling. As the score,  $\mathcal{L}_{D_i}$ , of each discriminator is computed independently before applying the average operation, the hinge loss in Eq. 2 will prevent optimization through those discriminators that perform classification correctly, and refrain individual discriminators from contributing too large or small scores. In fact, applying an extra average pooling layer to the final layer of the discriminator network is equivalent to converting the final fully connected layer to having 1-dimensional output, i.e. the architecture of one discriminator without any ensemble, which is also susceptible to overfitting (see Section 6.7).

## 5 DYNAMIC CONTROLLER LEARNING

Following the GAIL framework, we train action policies as dynamic controllers via reinforcement learning without having to manually design a reward function. Instead, we exploit the discriminator output as the reward signal.

### 5.1 State and Action Space

State-of-the-art imitation learning implementations for physics-based character control typically construct the state space by leveraging the target pose implicitly through a phase variable [Holden et al. 2017; Peng et al. 2018] or explicitly [Bergamin et al. 2019; Park et al. 2019; Won et al. 2020] by using the target pose directly or the deviation between the target and the current pose of the character. When employing such a kind of action policies for interactive control, the system needs to be able to generate a target pose [Lee et al. 2019] or find a proper one from the reference motion dataset [Clavet 2016; Holden et al. 2020]. Such a process, though, could be time consuming. In contrast, in our framework, the policy network performs target pose inference based on a small number of previously encountered frames (similar to the observation space outlined in Section 4.1), and directly outputs target postures that are given as input to PD servo controllers.

As opposed to the discriminator, action policies need to generate reasonable target posture depending not just on the character pose but also on the current velocity. Therefore, we augment the observation space and set the state space for action policies as  $\mathbf{s}_t := \mathbf{o}_{t-3:t}^{+v} \in \mathbb{R}^{4 \times 13|\mathcal{B}|}$ , where  $\mathbf{o}_{t-3:t}^{+v}$  is the augmented observation based on four consecutive frames from  $t - 3$  to  $t$  (inclusive) containing also the velocity state of character body links relative to the root heading direction at the  $t$ -th frame. We use a recurrent neural network (RNN), a GRU [Chung et al. 2014] layer in our implementation, to embed the input state defined in the temporal space.

The action space is the target posture for each joint and serves as the control signal fed to the PD servos. For revolute joints, the 1-dimensional target posture denotes the desired angle position in radians. For spherical joints, the target posture is a 4-dimensional rotation expressed in the format

of axis and angle. The action policy is defined by a normal distribution with dependent components, the mean value of which and the logarithm of the standard deviation are obtained from the output of the policy network.

## 5.2 Behavior Learning

We combine our discriminator learning approach with a policy gradient algorithm for reinforcement learning to find an imitation policy  $\pi$  that maximizes the cumulative reward  $\sum_t \gamma^{t-1} r_t(s_t, a_t, s_{t+1})$  of collected experiences where  $\gamma$  denotes the discount factor. We compute the reward,  $r_t$ , for each state-action-state transition by considering the average score of the ensemble of  $N$  discriminators. The score from each discriminator is clipped before averaging according to hinge loss definition in Eq. 2, which avoids biasing the reward towards too low or small scores from individual discriminators:

$$r_t(s_t, a_t, s_{t+1}) = \frac{1}{N} \sum_{i=1}^N \text{clip}(D_i(\mathbf{o}_{t-3:t+1}), -1, 1). \quad (5)$$

Given the state-observation pair  $\{(s_t, s_{t+1}); \mathbf{o}_{t-3:t+1}\}$ , this reward evaluates the agent's performance to reach a desired target pose at frame  $t+1$  given the character's trajectory from frame  $t-3$  to  $t$ .

During training, by interpolating the keyframes, a pose randomly drawn from the reference motion is used to initialize the character model in each episode. The interpolation prevents the discriminators from simply memorizing the poses in the keyframes, and helps the policy for character control to generalize better. After pose initialization, at each time step  $t$ , the agent receives the reward signal  $r_t$  from the discriminator ensemble. An episode ends if the time step reaches the maximal length of the reference motion clip for a non-cyclic motion, or if an overtime limit, 500 frames in our implementation, is hit for a cyclic motion. An early termination is taken if an unexpected contact between the character body link and the ground occurs, e.g., if the character falls down and gets in contact with the ground with its chest link when imitating the walk motion. The policy is updated, through a reinforcement learning algorithm, which is DPPO [Heess et al. 2017] in our implementation, after a batch of state-action-reward samples is collected. The ensemble discriminator is trained together with the policy using observation samples collected from the agent under training and the same amount of samples drawn from the reference motion. Algorithm 1 summarizes the training process using our GAN-like approach.

Our approach can be easily extended for *integrated learning* of a single policy from multiple reference motion clips, i.e., training one policy capable of imitating pose trajectories from a collection of multiple reference clips. To do so, at the beginning of each training episode, we randomly choose one of the clips from the collection of target, reference clips for imitation. Such an approach can simplify the interactive system for character control, which we will introduce in Section 5.3, as we can use a single policy to enable the character to automatically perform different behaviors according to its current pose when a policy switch is triggered.

## 5.3 Interactive Policy Switch

At runtime, there is only one action policy activated that controls the character by outputting target postures to PD servos. Our system allows for interactive character control by letting the user specify a target action policy that can take over the character and perform a specific behavior. If the target policy can imitate its corresponding reference motion well, when the current pose of the character is similar to some pose in the reference motion, the target policy should be able to take over the character and perform the behavior shown in the reference motion. Based on this assumption, by exploiting the ensemble of discriminators trained in tandem with the policy network, we use the discriminator score to implicitly estimate the similarity of the current pose

**Algorithm 1:** GAN-like approach for imitation learning

---

```

Initialize action policy network  $\pi$ ;
initialize policy replay buffer  $\mathcal{T}$ ;
initialize discriminators network  $D_i$  where  $i = 1, \dots, N$ ;
initialize discriminator replay buffer  $\mathcal{M}$ ;
preprocess reference motion dataset  $\mathcal{K}$ ;
initialize simulation environment.
while training does not converge do
  for each environment step  $t$  do
     $\mathbf{a}_t \sim \pi(\mathbf{s}_t)$  ;
     $\mathbf{s}_{t+1}, \mathbf{o}_{t-3:t+1} \leftarrow$  environment updates with character control signal of  $\mathbf{a}_t$ ;
    compute  $r_t$  using Eq. 5;
    draw the sample  $\tilde{\mathbf{o}}_{t-3:t+1}$  from  $\mathcal{K}$ ;
     $\mathcal{M} \leftarrow \mathcal{M} \cup \{\mathbf{o}_{t-3:t+1}, \tilde{\mathbf{o}}_{t-3:t+1}\}$ ;
     $\mathcal{T} \leftarrow \mathcal{T} \cup \{(\mathbf{s}_t, \mathbf{a}_t, r_t, \mathbf{s}_{t+1})\}$ ;
     $\mathbf{s}_t \leftarrow \mathbf{s}_{t+1}$ .
  end
  for each discriminator update step do
    | update ensemble discriminator  $D$  based on Eq. 4 using samples from  $\mathcal{M}$ .
  end
   $\mathcal{M} \leftarrow \emptyset$ .
  for each policy update step do
    | update  $\pi$  using samples from  $\mathcal{T}$ .
  end
end

```

---

trajectory  $\mathbf{o}_{t-4:t}$  to segments in the reference motion of the target policy, and consider the switch to the target policy to be feasible if

$$\frac{1}{N} \sum_{i=1}^N \text{clip}(D_i^{\text{target}}(\mathbf{o}_{t-4:t}), -1, 1) \geq \tau, \quad (6)$$

where  $D_i^{\text{target}}$  is the  $i$ -th discriminator of the target policy and  $\tau$  is a threshold scalar value.

As detailed in Section 5.1, policy networks perform imitation by causal inference based only on the character's last pose trajectory. Therefore, when performing policy switch, we do not need to explicitly generate a target pose or track the reference motion by keyframes or a phase state variable, which decreases the runtime cost of the interactive system. In addition, the transitioning between poses from different behaviors can happen at the intermediate states between keyframes, as the discriminators are trained using interpolated keyframe samples from the reference motion instead of simply memorizing the keyframes. To improve the robustness of policy switch between motions having similar but not exactly the same poses, we add some noise to the character's initial pose at each training episode and also to the corresponding samples drawn from the reference motion for discriminator learning.

After receiving a control signal, our system keeps checking the switch condition shown in Eq. 6 at each frame, and sets the target policy as the current policy if the condition is met or ignores the control signal if the condition cannot be satisfied within an acceptable response time. Our approach only relies on pre-trained policies to control the character performing specific behaviors, and does not generate any transient states during the running time of policy switch. Therefore, to expect a

Parameter	Value
policy network learning rate	$5 \times 10^{-6}$
value network learning rate	$1 \times 10^{-4}$
discriminator learning rate	$1 \times 10^{-5}$
reward discount factor ( $\gamma$ )	0.95
GAE discount factor ( $\lambda$ )	0.95
surrogate clip range ( $\epsilon$ )	0.2
gradient penalty coefficient ( $\lambda^{GP}$ )	10
PPO replay buffer size	4096
PPO batch size	256
PPO optimization epochs	5
discriminator replay buffer size	8192
discriminator batch size	512

Table 1. Hyperparameters

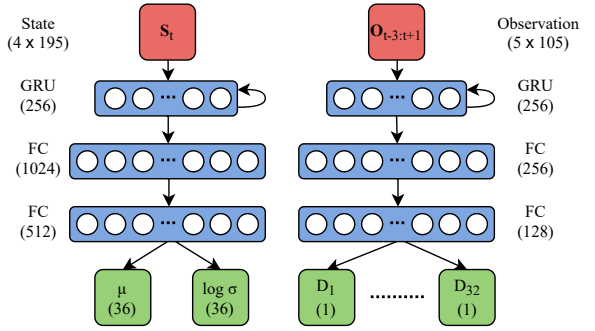


Fig. 4. Policy and discriminator network architecture.

transition from one motion to another to be feasible during runtime, system designers must ensure that the two motions have similar poses. Motion matching [Bergamin et al. 2019; Clavet 2016; Holden et al. 2020] technique can be employed as a method to perform similarity check between two motion clips during the data preprocessing phase.

## 6 EXPERIMENTS

In this section, we experimentally evaluate our work focusing on two aspects: 1) the motion imitation ability of policies trained by our GAN-like approach; and 2) the effectiveness of the implemented interactive control system that exploits the trained policies. We also perform sensitivity analysis on the learning performance using different discriminator training strategies.

### 6.1 Setup

We set up our simulation environment using PyBullet [Coumans and Bai 2021]. In all our experiments, we use a humanoid character that is 1.62m tall and weights 45kg. The simulated character has 8 spherical joints and 4 revolute joints, plus 2 end-effectors (hands) connected to the forearms with fixed joints and a root link, resulting in 15 body links with 34 degrees of freedom in total. The character is controlled through stable proportional derivative controllers [Tan et al. 2011]. The whole system interacts with user input and queries character control signals from the policy network at 30 Hz, while running forward dynamics simulation at 600 Hz. We model the control signal for each spherical joint to the PD servos as a quaternion resulting in a 36-dimensional action space. As described in Sections 4.1 and 5.1, the policy network takes as input four consecutive frames with state space of  $\mathbb{R}^{4 \times 195}$ , while the observation space for discriminators is  $\mathbb{R}^{5 \times 105}$ .

In our experiments, we employ 8 threads to perform distributed training under the framework of DPPO [Heess et al. 2017], and use Adam optimizer [Kingma and Ba 2014] to perform policy optimization. DPPO uses an actor-critic architecture to perform reinforcement learning. The policy (actor) network has one GRU layer with 256 hidden neurons to embed the temporal state input, followed by 2 fully-connected (FC) layers with hidden neurons of 1024 and 512 respectively. We use a multivariate Gaussian distribution with independent components as the policy distribution. The policy network outputs the mean and standard deviation parameters of the policy distribution. The value (critic) network is trained to estimate the state value function, and has the same architecture with 1-dimensional output. We setup multiple discriminators sharing the same feature extraction layers, which have similar architecture with the policy network but use fully-connected layers with 256 and 128 neurons following the GRU layer. By default, we use an ensemble of 32 discriminators

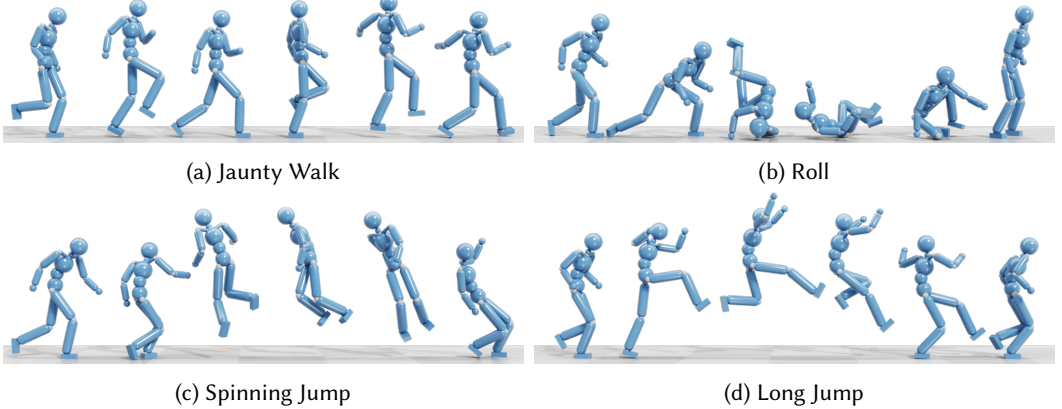


Fig. 5. Motion poses captured from the policies trained by our GAN-like approach. Table 2 gives a description of these motions. We refer to the supplemental video for more examples.

initialized randomly. Discriminator weights are initialized by orthogonal initializer [Saxe et al. 2013]. The policy network is initialized by truncated normal distribution with a small value of standard deviation 0.05 to prevent too large output at the early training. Input state and observation to the networks are normalized by a moving average that is dynamically updated during training. All the hyperparameters and network architecture are shown in Table 1 and Fig. 4, respectively.

## 6.2 Data Acquisition

All reference motion clips used in our experiments are extracted from the LAFAN1 dataset [Harvey et al. 2020]. The motion data provided by LAFAN1 are captured from different subjects at 30Hz. Each data item contains a motion capture recording, typically having a length of 3-5 minutes, with varieties of behaviors under a common motion category performed by one subject. We synthesize a short reference motion clip (1-3s) by extracting a motion segment of an interesting single behavior from consecutive frames recorded in a data item, and retarget the local joint position from the motion data to our character model without any manual reprocessing. We demonstrate that our approach can work well with raw motion capture data, even when the character model does not match perfectly the recorded subjects. Table 2 gives a description of the behaviors contained in the reference motion clips used in our experiments. We refer to the supplementary document for details of all the reference motion clips that we used for policy training during experiments.

## 6.3 Motion Clip Imitation

We show motion pose snapshots captured from some of our trained imitation policies in Fig. 5. All policies were trained on a single machine with Intel 6148G CPU and Nvidia V100 GPU. It takes about 12 hours to train a policy using a fixed budget of 20 million samples (environment steps).

To quantitatively evaluate the imitation ability of our GAN-like approach, we measure the imitation error as the average global position error of character body links compared to the reference motion:

$$e = \frac{1}{|\mathcal{B}|} \sum_{i \in \mathcal{B}} \|p_{i,t} - p_{i,t}^{ref}\|_2, \quad (7)$$

where  $\mathcal{B}$  is the collection of character body links,  $p_{i,t}$  is the 3D global position of the  $i$ -th link at frame  $t$  and  $p_{i,t}^{ref}$  is the position of the corresponding link in the reference motion. Since our

Motion	Length [s]	Imitation Error [m]	Description
walk	1.10	$0.06 \pm 0.02$	normal walking with a speed around 1.2m/s
pace	1.70	$0.11 \pm 0.04$	slow walking with arms akimbo
limp	1.90	$0.09 \pm 0.06$	slow walking with right leg hurt
swaggering walk	1.07	$0.05 \pm 0.01$	exaggerated walking with one arm akimbo
sashay walk	1.07	$0.04 \pm 0.02$	walking in a slightly exaggerated manner
jaunty walk	1.40	$0.15 \pm 0.07$	walking in a spirited manner
stomp walk	1.23	$0.05 \pm 0.04$	walking while stomping on the ground
stoop walk	0.93	$0.05 \pm 0.02$	slow walking with body bent over
joyful walk	1.20	$0.08 \pm 0.03$	strut walking rhythmically
walk with arms akimbo	2.20	$0.10 \pm 0.08$	high knee walking with arms akimbo
sharp turn during running	1.47	$0.30 \pm 0.05$	90-degree sharp turning during running
90-degree turn during walking	2.07	$0.10 \pm 0.04$	90-degree turning during a normal walk
roll	3.37	$0.26 \pm 0.06$	forward rolling from a standing pose
fight stance	0.87	$0.05 \pm 0.01$	standing with a fighting pose
run	2.37	$0.10 \pm 0.04$	running starting from a walking pose
spinning jump	3.00	$0.16 \pm 0.04$	jumping and spinning the body in the air
long jump	1.77	$0.21 \pm 0.07$	jumping after a running approach
get up	2.87	$0.21 \pm 0.03$	getting up from stumbling
punch	1.73	$0.09 \pm 0.06$	left and then right straight punch
kick	2.33	$0.14 \pm 0.06$	side kick

Table 2. Imitation performance when learning from a single motion clip. Reported numbers denote mean values over 20 trials  $\pm$  standard deviation.

Motion Collection	# of clips	Length [s]	Imitation Error [m]	Description
run	2	4.73	$0.15 \pm 0.05$	running starting from walking poses with different standing foot
spinning and long jump	4	9.53	$0.37 \pm 0.19$	spinning jump and long jump with different take-off foot
get up	5	13.7	$0.18 \pm 0.06$	getting up from stumbling with different poses lying on the ground
punch	3	4.77	$0.12 \pm 0.10$	punches with different stance
kick	4	8.43	$0.13 \pm 0.11$	kicks with different stance

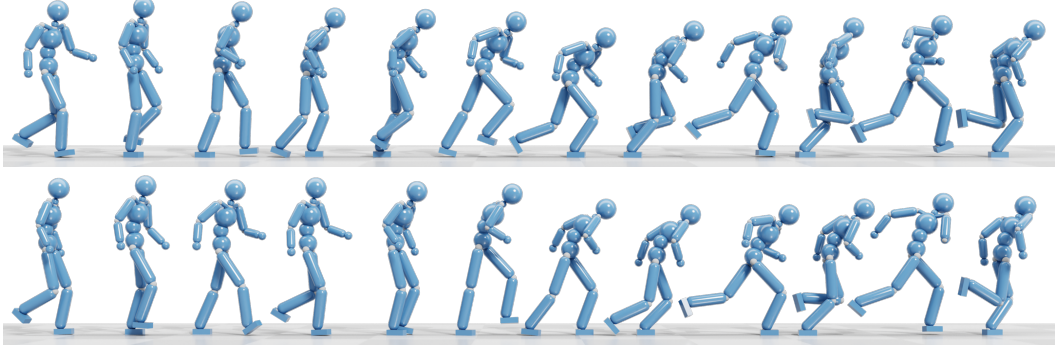
Table 3. Imitation performance of policies learning from multiple reference clips in a collection. Each collection has different behaviors under the same category of motions. A single policy is trained in an integrated manner to learn all the behaviors in one collection. Results are the evaluation over 20 trials of each clip that a policy learns to imitate.

approach does not implicitly employ any target pose or explicitly exploit any time component or phase state to perform synchronization with the reference motion, a small pose error caused by desynchronization occurring at early frames may result in a large accumulated error even if the subsequent motion is performed smoothly. To synchronize the motion gaits, we compute the error of one motion cycle and perform multiple test trials starting at different initial poses. Table 2 lists all the reference motion clips used in our experiments for single-clip imitation tests and the corresponding imitation errors obtained with our approach. Our approach can imitate the reference motion closely without requiring any explicit reward function fine-tuning.

Besides single-motion clip imitation, our approach can also train a policy in an integrated manner to imitate motions from multiple clips (Table 3). As such, we can control the character to execute different behaviors automatically according to the initial pose given to the policy that takes over the



(a) Diverse punch behaviors, given different initial stances, performed by a single policy learned from reference clips in the “punch” collection (Table 3).



(b) Diverse transitions from walking to running performed by a single policy learned from reference clips in the “run” collection (Table 3).

Fig. 6. Diverse behaviors exhibited by one policy learned from a collection of reference clips in an integrated manner. The policy can automatically decide which behavior from the reference clips should be taken based on the given initial pose.

character. For example, one policy can control the character to perform different kinds of punches according to the character’s stance, as shown in Fig. 6a. In Fig. 6b, a single policy, learned from two reference clips of running motion starting with a different foot on the ground, allows the character to perform flexible walk-to-run transitions.

When the same number of samples is exploited for training, learning from multiple clips in an integrated manner exploits only a part of those samples to train each distinct behavior. The difficulty of learning, therefore, would increase if poses from these clips are quite distinct. For example, the clips used in the “run” collection have similar poses during the running phase, and the policy only needs to learn two different transitions besides running (walk to run starting with the left and starting with the right foot on the ground, respectively). In contrast, motions in the “spinning and long jump” collection, differ a lot to each other, as shown in Fig. 5, and the imitation error increases compared to the corresponding single-motion clip imitation. In our experiments, the largest collection for single policy training contains five clips of “get up” motions with different poses lying on the ground, having a total length of 13.7s (411 frames). The trained controllers can imitate different behaviors in all the five clips with a small error, as shown in Table 3.

#### 6.4 Robustness

We evaluate the policy robustness through projectile testing. During the test, at each frame, a cube with fixed mass is launched towards a uniformly sampled location on the torso of the character, which is controlled by the “walk” policy. All cubes have a side length of 0.2m and an initial velocity of 0.2m/s. We consider a control policy to fail if the character falls down and keeps lying on the

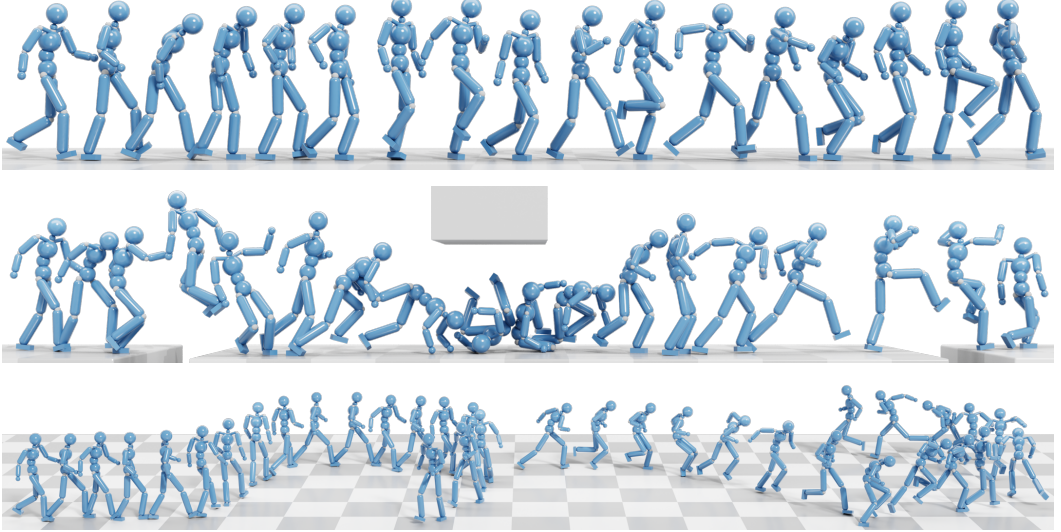


Fig. 8. Interactive control of a physically simulated character using our approach. Responding to the user's input, the character (from top to bottom) walks with varying styles, navigates through a challenging terrain, and changes heading direction.

ground for 10 consecutive frames. For comparisons, we employ a policy trained by motion tracking using the approach from Peng et al. [2018] as a baseline. Figure 7 reports the time, in the term of the number of frames, that a policy can control the character before failure while varying the mass of the cube. Solid lines report the average performance over 1,000 trials and shaded regions indicate the standard deviation. All policies are obtained without projectile training. By controlling the character dynamically based on the last pose trajectory, our approach achieves better robustness performance compared to the baseline algorithm, which keeps tracking the reference motion with a fixed time interval between frames without consideration of the current pose of the character.

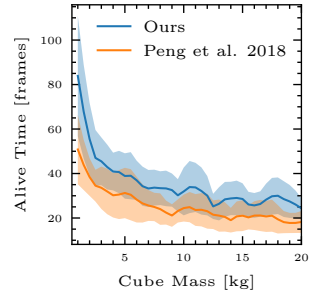


Fig. 7. Policy robustness test.

## 6.5 Interactive Control

Our approach allows for interactive character control by taking user control input and performing policy switch based on the average score provided by the ensemble discriminator of the target policy, as described in Section 5.3. Figure 8 shows examples of policy switch interactively responding to external control signal provided by the user. Please see the supplemental video for more examples.

Besides being a system passively responding to user control input, our interactive control scheme can also work actively by setting up a recovery policy to check and, if necessary, temporally take over the character. Figure 9 shows a get-up policy working as a recovery policy to help a fallen down character get back to walking. The get-up policy keeps checking the character state by querying the score from its discriminators at each frame. It is activated automatically when the score is greater than a threshold value, and returns the control back to the "walk" policy if the ensemble discriminator from the "walk" policy gives a score high enough.

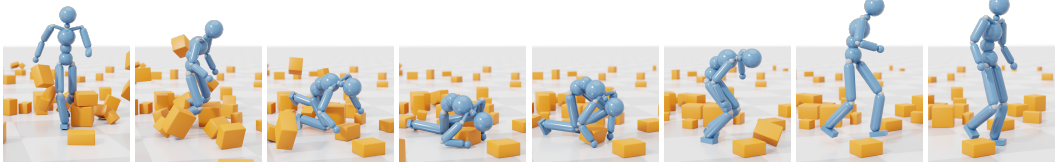


Fig. 9. Auto-activated recovery policy. A get-up policy works as a recovery policy activated automatically to help a fallen down character to get back to walking. The get-up policy is obtained by learning from reference clips in the “get up” collection integratedly (Table 3).

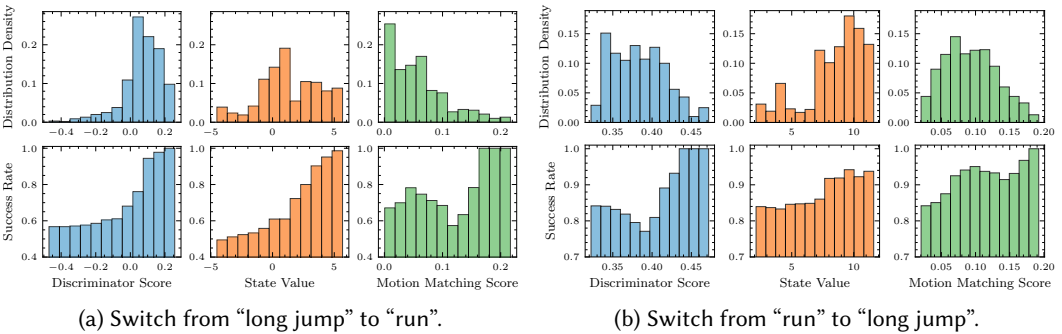


Fig. 10. Evaluating different metrics for policy switch. The top row reports the distribution of scores/values per metric obtained when the target policy evaluates the character poses controlled by the source policy. The bottom row reports the success rate of policy switch for different scores/values used as the switch threshold.

*Transition Test.* To evaluate the performance of the ensemble discriminator score during interactive control, we run 10,000 tests of policy switching from the “long jump” policy to the “run” policy. In each trial, the character is initially controlled by the “long jump” policy with a pose randomly sampled from the reference clip. We consider the switch to be successful if the “run” policy can take over during the long jump motion allowing the character to safely perform running. Figure 10a shows the corresponding score distribution and provides statistics on the success rate when different discriminator scores are used as a decision threshold to perform policy switch. We also report the results of policy switch from “run” to “long jump” in Fig. 10b. As shown in the figures, when facing unseen poses from the other motion, the discriminator ensemble still provides a reliable measurement to reflect the success rate of policy switch.

As a comparison, we employed the value network in our DPPO implementation and used the state value to perform policy switch check, with the corresponding results shown in Fig. 10. The state value provides an estimation of the accumulated reward, which is actually the discriminator score (Eq. 5 and 6), and can reflect the policy switch success rate. Our implementation, though, directly uses the discriminator score to perform policy switch check, as we find that a higher state value cannot always guarantee a higher success rate, for example, during the switch from the “run” policy to “long jump”. In Fig. 10a, we also report the policy switch performance when using the inverse of motion matching cost [Clavet 2016] as a similarity score. The issue with this approach is that the sample coverage rate decreases too much as the chosen threshold value increases. This means that when a high motion matching score is chosen as the decision threshold to guarantee successful transitions, a large portion of valid policy switches could be denied. We refer to the supplementary document for more results about the success rate of policy switch in various scenarios.

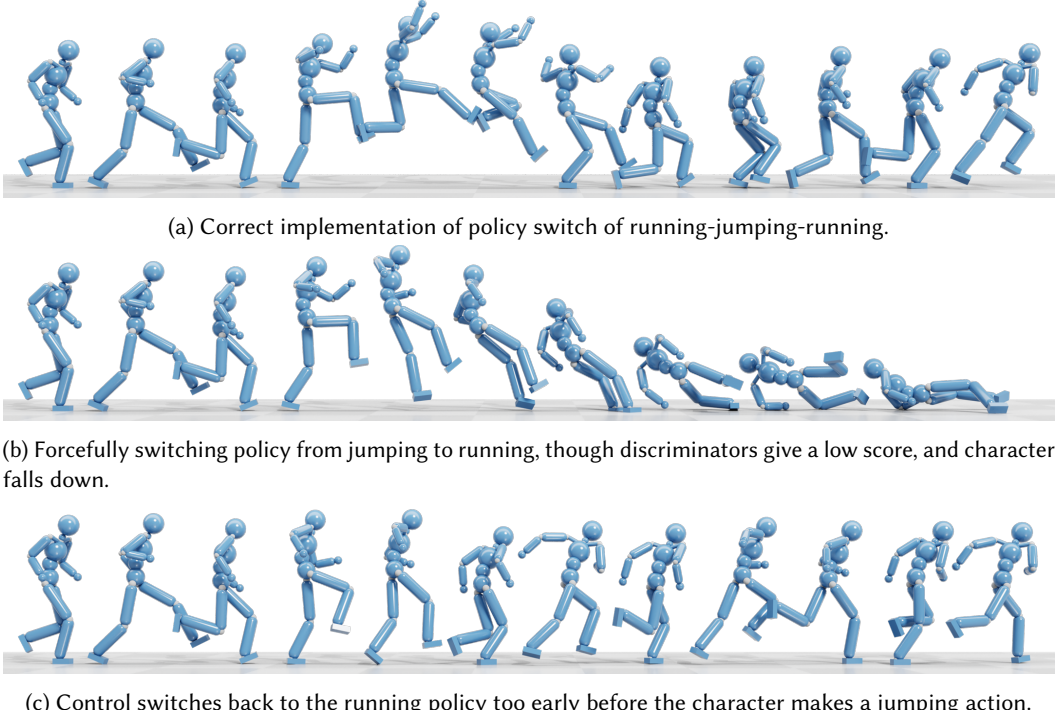


Fig. 11. Failure case study of policy switch between running and jumping.

*Failure Case Study.* Policy switch typically fails due to two reasons. The first is that the target policy fails to control the character given its current pose. The character under such a case would fall down and be unable to recover, as, e.g., shown in Fig. 11b where we force a policy switch to happen with a low score value. This issue can be solved by choosing a proper threshold value to indicate if the switch is possible, which can be behavior specific. For example, as shown in Fig. 10, a threshold value of the discriminator score of 0.1 can be chosen to ensure a success rate over 95% when switching policy from jumping to running; and to guarantee a safer switch, the threshold value can be chosen as 0.2. The second kind of failure is that a target policy takes over the character before the current policy finishes its expected action. This is not a real issue, if the target policy simply takes over as fast as possible responding to the user’s control input. However, it could be a problem when we need the policy switch to occur *after* a specific action done. For example, as shown in Fig. 11a, after the character performs a jump, we would like to automatically switch the control policy back to running. If we query the discriminators of running policy right after the jumping policy takes over, the discriminators will give a higher score, since the character is still in the pose of running; and, hence, the control policy will switch back to running without the character performing any jump action, Figure 11c shows an example of such a failure. This issue can be addressed by introducing frame delays between policy switches. For example, given that the long jump motion has 43 frames in total, after its corresponding policy takes over the character, we can set a delay of 20 frames before the system calls on other policies. As such, the long jump policy has enough time to let the character perform a jump before any other policy takes over.

## 6.6 Runtime Cost

We test models trained using our approach on a common consumer-level computer with Intel i7-7700K CPU and GeForce 1080Ti GPU and report the runtime cost in Table 4. The listed number of parameters and model size are for a single control policy and an ensemble of 32 discriminators. The forward runtime reports the average time over 1,000 trials that it takes to perform a forward pass

on the policy network and the discriminator network, respectively, of each of the five controllers shown in Table 3. As described in Section 6.1, our approach uses a fixed network architecture for each controller, and thus each policy and the corresponding ensemble discriminator have a fixed model size, which is unrelated to training data set, i.e., the length and the number of reference clips that a policy is trained to imitate. The total memory usage will increase linearly with the number of controllers employed in one scenario. Even though the ensemble of discriminators has a smaller memory footprint than the policy, it requires a bit more time for a forward pass because the observation space has one extra temporal dimension compared to the state space.

## 6.7 Ablation Studies

We perform ablation studies on various design decisions of our GAN-like approach using two challenging tasks: spinning jump and long jump. Spinning jump requires the character to keep balance well in the air and spin its body correctly. The long jump task has a demand on the jump distance and height, as the imitation error is measured by the global positions of body links. As shown in Table 2, the trained policies perform relatively worse in these two tasks, compared to the policies for other control tasks.

Figure 12 focuses on the gradient penalty loss term for discriminator training, and compares the imitation error during training to two baselines: the work from Peng et al. [2018] that relies on motion tracking and the work from Merel et al. [2017] that uses GAIL with observations as the input to the discriminator. As it can be seen, our approach can achieve comparable performance to the state-of-the-art baseline from Peng et al. [2018] that has a carefully designed reward function to facilitate imitation learning. Training a physics-based humanoid character controller using the method from Merel et al. [2017] typically needs hundreds of millions of samples, and cannot work effectively within 20 million of samples. When no gradient penalty is used with our approach (“w/o GP”), the discriminators can easily identify samples from the character agent. Hence, the policy network always receives a very low reward signal and hardly learns anything useful.

Figure 13a shows the performance when different observation spaces are used for discriminator training. By default, our approach uses as the observation space the position and orientation of character body links from the last 4 consecutive frames, in the local system defined by the root position and orientation of the last frame. As it can be seen, the introduction of velocity either from links (Link + Vel) or joints (Joint + Vel) could increase the difficulty of training. It is relatively hard for the policy to control the immediate link or joint velocity through a PD servo in order

	Policy Network	Discriminators
# of Parameters	1,154,730	381,810
Model Size	4.62 MB	1.53 MB
Forward Runtime	$189.52 \pm 8.71\mu\text{s}$	$193.53 \pm 5.61\mu\text{s}$

Table 4. Runtime cost of single policy and discriminator ensemble networks.

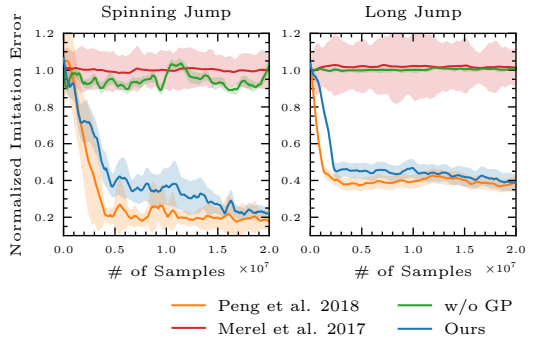


Fig. 12. Gradient penalty ablation study. Colored regions denote mean values  $\pm$  a standard deviation based on 20 trials.

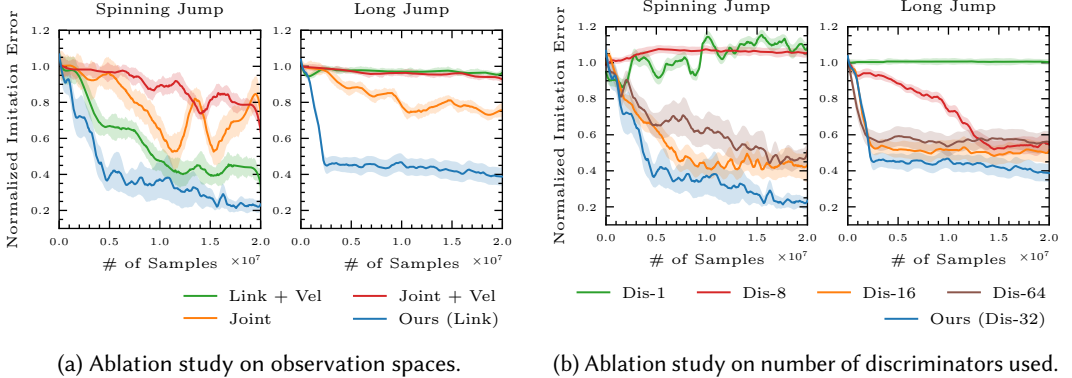


Fig. 13. Effect that different observation spaces and number of discriminators have on the learning performance. (a) Link + Vel uses the link velocity besides just the position and orientation as the observation space for the discriminators. The Joint space uses the local joint pose plus the root position and orientation, with the Joint + Vel also including the joint and root velocity. (b) Dis- $N$  denotes the case of training  $N$  discriminators simultaneously for reward generation.

to meet the reference velocity computed from the pose difference between two keyframes in the reference motion. Therefore, discriminators can distinguish character pose trajectories from the reference motion easily based on velocity terms, and generate quite low reward signals, even though the pose trajectories are visually similar. As for the visual performance, the introduction of velocity is redundant, since the visual velocity can be inferred from character poses in consecutive frames. The observation space that employs local joint poses (Joint) provides worse performance compared to our approach that uses the link positions. Discriminators in the local joint case could be fooled by the policy network and cannot distinguish samples from the reference motion effectively. This is due to the fact that the error between joint poses measured by rotation angle for revolute joints and quaternion for spherical joints is typically small, even though the overall character poses are visually quite different.

In Fig. 13b, we compare the training performance when different number of discriminators are employed. As shown in the figure, the policy network with 1 discriminator and that with 8 discriminators cannot be trained effectively. The more discriminators are used, the harder the ensemble discriminator training will be. This avoids overfitting during the early stage of training where the character agent performs largely differently to the reference motion, and helps solve the problem of vanishing reward signal. On the other hand, the increased difficulty in discriminator optimization prevents the discriminators from effectively identifying small errors between the character poses and the reference motion, as shown in the 64 discriminators case. We use an ensemble of 32 discriminators to balance the trade-off between overfitting and underfitting.

## 7 DISCUSSION AND FUTURE WORK

We propose a GAN-inspired approach combined with reinforcement learning to perform imitation learning for physics-based character control without requiring any explicit design of a reward function. In our approach, policies perform inference and control the character through short-term pose trajectories, eliminating the need to indicate the target keypose that it should follow. Based on this approach, by exploiting the discriminator to measure the similarity between the character's pose and the reference motion, we implement an interactive control system for policy switch during character control according to external user-input signals. Although, we empirically demonstrated

that our approach can perform imitation learning and interactive control effectively, there are still some limitations that we would like to address in the future.

*Motion transition quality.* In our experiments, the reference clips are extracted from the LAFAN1 dataset (Section 6.2) and are typically discontinuous to each other. Each control policy only learns to imitate behaviors from its own collection of reference clips, and is not fine-tuned to adapt to any pose in other clips. Consequently, this could often lead to nonsmooth transitions during policy switch, or even make an expected transition unfeasible because there are no similar poses in the reference motions of the two policies. In practice, this issue can be addressed by explicitly providing the transition motions, which can be obtained from motion capture or in-between motion generation techniques [Harvey et al. 2020], and using them as reference motions for the controller policies to imitate. An alternative solution is to force a transition stage in training, during which the character is initialized using poses from other motions [Bergamin et al. 2019].

*Unweighted observations.* In our framework, discriminators distinguish character pose samples from the reference motion via root-related link positions and orientations, and rely on these observations to provide reward signals for policy training. A manually designed reward function for imitation learning [Bergamin et al. 2019; Peng et al. 2018; Won et al. 2020] would typically consider the contributions that different body links or joints make for specific behaviors, and assign different weights to those link- or joint-related errors when computing the reward. However, in our current implementation, the observations are unweighted. This could cause issues when the policy gives a higher priority during optimization to attenuate the pose error related to some trivial body links or joints, which have less impact on visible differences between target poses.

*Long-term memory.* As the policy network relies on the poses from the last four frames to perform inference and character control, it lacks the ability of long-term memory. When facing complex motions or learning from multiple motion clips, the policy network may fail to learn the diversity of motions if there are some fairly similar short-term pose trajectories in the reference motions leading to different following poses. An obvious solution would be to increase the number of poses used to construct the state space. However, this could increase the difficulty of learning as the inference would be disturbed by more noises in the trajectory.

*Importance sampling.* Our approach can learn diverse behaviors from multiple motion clips. In each training episode, we initialize the character randomly by uniformly picking a pose from those clips. A more effective way of training should take into account the current performance of the policy, and do an importance sampling when initializing the character pose. In such a way, the policy under optimization can dedicate more training to the behaviors that it performed relatively worse, and thus exploit samples more efficiently. Park et al. [2019] use an adaptive sampling method, dividing the reference motion into  $n$  segments and initializing the character pose by drawing samples from the segments based on the distribution of state value. In our approach, we can employ the discriminator score as a more accurate estimation of the performance of the policy under training, and do importance sampling.

*Goal-conditioned learning.* In interactive control experiments (Section 6.5), we only consider the case of switching policies according to external control signals. To achieve a truly interactive control policy that is responsive to user input, such as a walking or running policy with interactive speed or heading direction adaption, we can implement goal-conditioned policy learning by introducing a dynamic goal state during training [Bergamin et al. 2019; Peng et al. 2017; Xie et al. 2020]. A goal-conditioned reward function combining our GAN-like approach can be set up as

$$r_t = w_{goal} r_{goal}(\mathbf{s}_t, \mathbf{g}_t, \mathbf{a}_t, \mathbf{s}_{t+1}) + w_{GAN} r_{GAN}(\mathbf{s}_t, \mathbf{a}_t, \mathbf{s}_{t+1}), \quad (8)$$

where  $r_{goal}$  is the reward related to the goal completion having a dynamic goal state  $g_t$ ,  $r_{GAN}$  is the reward from our GAN-like approach (Eq. 5), and  $w_{goal}$  and  $w_{GAN}$  are coefficients to balance the weights of the two reward components.

As we highlight above there are a number of improvements that can be made to further increase the performance and general applicability of our proposed work. Based on our current results, we feel that there are several possible applications of our framework in production games and interactive applications as i) it does not require any explicit reward design to learn control policies, ii) it allows for interactive policy switch during character control based on external input signal at a low runtime cost, and iii) it is easy to be extended to support more action policies. Of course, a preprocessing step is required to gather reference motions. However, we can argue that a technique similar to motion matching can be employed before training to quickly determine whether multiple reference trajectories can be combined to learn an interactive control policy that can support different behaviors. While future research is also needed to guarantee the motion quality of controller transitions, we believe that, overall, our proposed framework provides a simple and flexible alternative for imitation learning and real-time control of physically simulated characters.

## REFERENCES

- Kevin Bergamin, Simon Clavet, Daniel Holden, and James Richard Forbes. 2019. DReCon: data-driven responsive control of physics-based characters. *ACM Transactions On Graphics* 38, 6 (2019), 1–11.
- Andrew Brock, Jeff Donahue, and Karen Simonyan. 2018. Large scale GAN training for high fidelity natural image synthesis. *arXiv preprint arXiv:1809.11096* (2018).
- David F Brown, Adriano Macchietto, KangKang Yin, and Victor Zordan. 2013. Control of rotational dynamics for ground behaviors. In *Proceedings of the 12th ACM SIGGRAPH/Eurographics Symposium on Computer Animation*. 55–61.
- Nuttapong Chentanez, Matthias Müller, Miles Macklin, Viktor Makoviychuk, and Stefan Jeschke. 2018. Physics-Based motion capture imitation with deep reinforcement learning. In *Proceedings of the 11th Annual International Conference on Motion, Interaction, and Games*. Association for Computing Machinery, Article 1, 10 pages.
- Junyoung Chung, Caglar Gulcehre, KyungHyun Cho, and Yoshua Bengio. 2014. Empirical evaluation of gated recurrent neural networks on sequence modeling. *arXiv preprint arXiv:1412.3555* (2014).
- Simon Clavet. 2016. Motion matching and the road to next-gen animation. In *Proc. of GDC*.
- Stelian Coros, Philippe Beaudoin, and Michiel van de Panne. 2010. Generalized biped walking control. *ACM Transactions on Graphics* 29, 4 (2010), 130.
- Erwin Coumans and Yunfei Bai. 2016–2021. PyBullet, a Python module for physics simulation for games, robotics and machine learning. <http://pybullet.org>.
- Danilo Borges da Silva, Rubens Fernandes Nunes, Creto Augusto Vidal, Joaquim B Cavalcante-Neto, Paul G Kry, and Victor B Zordan. 2017. Tunable robustness: An artificial contact strategy with virtual actuator control for balance. *Computer Graphics Forum* 36, 8 (2017), 499–510.
- Marco Da Silva, Yeuhi Abe, and Jovan Popović. 2008. Simulation of human motion data using short-horizon model-predictive control. *Computer Graphics Forum* 27, 2 (2008), 371–380.
- Thomas G Dietterich. 2000. Ensemble methods in machine learning. In *International workshop on multiple classifier systems*. Springer, 1–15.
- Ishan Durugkar, Ian Gemp, and Sridhar Mahadevan. 2016. Generative multi-adversarial networks. *arXiv preprint arXiv:1611.01673* (2016).
- Thomas Geijtenbeek, Nicolas Pronost, and A Frank van der Stappen. 2012. Simple data-driven control for simulated bipeds. In *Proceedings of the 11th ACM SIGGRAPH/Eurographics Symposium on Computer Animation*. 211–219.
- Thomas Geijtenbeek, Michiel van de Panne, and A Frank Van Der Stappen. 2013. Flexible muscle-based locomotion for bipedal creatures. *ACM Transactions on Graphics* 32, 6 (2013), 1–11.
- Ian J Goodfellow, Jean Pouget-Abadie, Mehdi Mirza, Bing Xu, David Warde-Farley, Sherjil Ozair, Aaron Courville, and Yoshua Bengio. 2014. Generative adversarial networks. *arXiv preprint arXiv:1406.2661* (2014).
- Ishaan Gulrajani, Faruk Ahmed, Martin Arjovsky, Vincent Dumoulin, and Aaron Courville. 2017. Improved training of Wasserstein GANs. *arXiv preprint arXiv:1704.00028* (2017).
- Perttu Hämäläinen, Joose Rajamäki, and C Karen Liu. 2015. Online control of simulated humanoids using particle belief propagation. *ACM Transactions on Graphics* 34, 4 (2015), 1–13.

- Félix G. Harvey, Mike Yurick, Derek Nowrouzezahrai, and Christopher Pal. 2020. Robust motion in-betweening. *ACM Transactions on Graphics* 39, 4 (2020).
- Nicolas Heess, Srinivasan Sriram, Jay Lemmon, Josh Merel, Greg Wayne, Yuval Tassa, Tom Erez, Ziyu Wang, SM Eslami, Martin Riedmiller, et al. 2017. Emergence of locomotion behaviours in rich environments. *arXiv preprint arXiv:1707.02286* (2017).
- Jonathan Ho and Stefano Ermon. 2016. Generative adversarial imitation learning. *arXiv preprint arXiv:1606.03476* (2016).
- Daniel Holden, Oussama Kanoun, Maksym Perekhchka, and Tiberiu Popa. 2020. Learned motion matching. *ACM Transactions on Graphics* 39, 4 (2020), 53–1.
- Daniel Holden, Taku Komura, and Jun Saito. 2017. Phase-functioned neural networks for character control. *ACM Transactions on Graphics* 36, 4 (2017), 1–13.
- Jemin Hwangbo, Joonho Lee, Alexey Dosovitskiy, Dario Bellicoso, Vassilios Tsounis, Vladlen Koltun, and Marco Hutter. 2019. Learning agile and dynamic motor skills for legged robots. *Science Robotics* 4, 26 (2019).
- Diederik P Kingma and Jimmy Ba. 2014. Adam: A method for stochastic optimization. *arXiv preprint arXiv:1412.6980* (2014).
- Taesoo Kwon and Jessica K Hodgins. 2010. Control systems for human running using an inverted pendulum model and a reference motion capture sequence. In *Proceedings of the 2010 ACM SIGGRAPH/Eurographics Symposium on Computer Animation*. 129–138.
- Taesoo Kwon and Jessica K Hodgins. 2017. Momentum-mapped inverted pendulum models for controlling dynamic human motions. *ACM Transactions on Graphics* 36, 1 (2017), 1–14.
- Seunghwan Lee, Moonseok Park, Kyoungmin Lee, and Jehee Lee. 2019. Scalable muscle-actuated human simulation and control. *ACM Transactions on Graphics* 38, 4 (2019), 1–13.
- Yoonsang Lee, Sungeun Kim, and Jehee Lee. 2010. Data-driven biped control. *ACM Transactions on Graphics* 29, 4 (2010), 129.
- Yoonsang Lee, Moon Seok Park, Taesoo Kwon, and Jehee Lee. 2014. Locomotion control for many-muscle humanoids. *ACM Transactions on Graphics* 33, 6 (2014), 1–11.
- Timothy P Lillicrap, Jonathan J Hunt, Alexander Pritzel, Nicolas Heess, Tom Erez, Yuval Tassa, David Silver, and Daan Wierstra. 2015. Continuous control with deep reinforcement learning. *arXiv preprint arXiv:1509.02971* (2015).
- Jae Hyun Lim and Jong Chul Ye. 2017. Geometric GAN. *arXiv preprint arXiv:1705.02894* (2017).
- Hung Yu Ling, Fabio Zinno, George Cheng, and Michiel Van De Panne. 2020. Character controllers using motion VAEs. *ACM Transactions on Graphics* 39, 4 (2020), 40–1.
- Libin Liu, Michiel van de Panne, and KangKang Yin. 2016. Guided learning of control graphs for physics-based characters. *ACM Transactions on Graphics* 35, 3 (2016), 1–14.
- Libin Liu, KangKang Yin, and Baining Guo. 2015. Improving sampling-based motion control. *Computer Graphics Forum* 34, 2 (2015), 415–423.
- Libin Liu, KangKang Yin, Michiel van de Panne, Tianjia Shao, and Weiwei Xu. 2010. Sampling-based contact-rich motion control. In *ACM SIGGRAPH 2010 papers*. 1–10.
- Josh Merel, Yuval Tassa, Dhruva TB, Sriram Srinivasan, Jay Lemmon, Ziyu Wang, Greg Wayne, and Nicolas Heess. 2017. Learning human behaviors from motion capture by adversarial imitation. *arXiv preprint arXiv:1707.02201* (2017).
- Takeru Miyato, Toshiki Kataoka, Masanori Koyama, and Yuichi Yoshida. 2018. Spectral normalization for generative adversarial networks. *arXiv preprint arXiv:1802.05957* (2018).
- Igor Mordatch and Emo Todorov. 2014. Combining the benefits of function approximation and trajectory optimization. In *Robotics: Science and Systems*, Vol. 4.
- Igor Mordatch, Emanuel Todorov, and Zoran Popović. 2012. Discovery of complex behaviors through contact-invariant optimization. *ACM Transactions on Graphics* 31, 4 (2012), 1–8.
- Masaki Nakada, Tao Zhou, Honglin Chen, Tomer Weiss, and Demetri Terzopoulos. 2018. Deep learning of biomimetic sensorimotor control for biomechanical human animation. *ACM Transactions on Graphics* 37, 4 (2018), 1–15.
- Andrew Y Ng, Stuart J Russell, et al. 2000. Algorithms for inverse reinforcement learning. In *International Conference on Machine Learning*, Vol. 1. 2.
- Soohwan Park, Hoseok Ryu, Seyoung Lee, Sunmin Lee, and Jehee Lee. 2019. Learning predict-and-simulate policies from unorganized human motion data. *ACM Transactions on Graphics* 38, 6 (2019), 1–11.
- Xue Bin Peng, Pieter Abbeel, Sergey Levine, and Michiel van de Panne. 2018. Deepmimic: Example-guided deep reinforcement learning of physics-based character skills. *ACM Transactions on Graphics* 37, 4 (2018), 1–14.
- Xue Bin Peng, Glen Berseth, KangKang Yin, and Michiel van de Panne. 2017. Deeploco: Dynamic locomotion skills using hierarchical deep reinforcement learning. *ACM Transactions on Graphics* 36, 4 (2017), 1–13.
- Xue Bin Peng, Erwin Coumans, Tingnan Zhang, Tsang-Wei Edward Lee, Jie Tan, and Sergey Levine. 2020. Learning agile robotic locomotion skills by imitating animals. In *Robotics: Science and Systems*.
- Xue Bin Peng, Ze Ma, Pieter Abbeel, Sergey Levine, and Angjoo Kanazawa. 2021. AMP: Adversarial motion priors for stylized physics-based character control. *ACM Transactions on Graphics* 40, 4, Article 1 (July 2021), 15 pages.

- Stuart Russell. 1998. Learning agents for uncertain environments. In *Proceedings of the eleventh annual conference on Computational learning theory*. 101–103.
- Andrew M Saxe, James L McClelland, and Surya Ganguli. 2013. Exact solutions to the nonlinear dynamics of learning in deep linear neural networks. *arXiv preprint arXiv:1312.6120* (2013).
- John Schulman, Sergey Levine, Pieter Abbeel, Michael Jordan, and Philipp Moritz. 2015a. Trust region policy optimization. In *International Conference on Machine Learning*. 1889–1897.
- John Schulman, Philipp Moritz, Sergey Levine, Michael Jordan, and Pieter Abbeel. 2015b. High-dimensional continuous control using generalized advantage estimation. *arXiv preprint arXiv:1506.02438* (2015).
- John Schulman, Filip Wolski, Prafulla Dhariwal, Alec Radford, and Oleg Klimov. 2017. Proximal policy optimization algorithms. *arXiv preprint arXiv:1707.06347* (2017).
- Jie Tan, Karen Liu, and Greg Turk. 2011. Stable proportional-derivative controllers. *IEEE Computer Graphics and Applications* 31, 4 (2011), 34–44.
- Yuval Tassa, Tom Erez, and Emanuel Todorov. 2012. Synthesis and stabilization of complex behaviors through online trajectory optimization. In *IEEE/RSJ International Conference on Intelligent Robots and Systems*. 4906–4913.
- Yuval Tassa, Nicolas Mansard, and Emo Todorov. 2014. Control-limited differential dynamic programming. In *IEEE International Conference on Robotics and Automation*. 1168–1175.
- Jungdam Won, Deepak Gopinath, and Jessica Hodgins. 2020. A scalable approach to control diverse behaviors for physically simulated characters. *ACM Transactions on Graphics* 39, 4 (2020), 33–1.
- Jungdam Won, Jungnam Park, and Jehee Lee. 2018. Aerobatics control of flying creatures via self-regulated learning. *ACM Transactions on Graphics* 37, 6 (2018), 1–10.
- Chun-Chih Wu and Victor Zordan. 2010. Goal-directed stepping with momentum control. In *Proceedings of the 2010 ACM SIGGRAPH/Eurographics Symposium on Computer Animation*. 113–118.
- Jia-chi Wu and Zoran Popović. 2010. Terrain-adaptive bipedal locomotion control. *ACM Transactions on Graphics* 29, 4 (07 2010), 72:1–72:10.
- Zhaoming Xie, Hung Yu Ling, Nam Hee Kim, and Michiel van de Panne. 2020. ALLSTEPS: Curriculum-Driven Learning of Stepping Stone Skills. *Computer Graphics Forum* 39 (2020), 213–224.
- KangKang Yin, Kevin Loken, and Michiel van de Panne. 2007. Simbicon: Simple biped locomotion control. *ACM Transactions on Graphics* 26, 3 (2007), 105–es.
- Wenhai Yu, Greg Turk, and C Karen Liu. 2018. Learning symmetric and low-energy locomotion. *ACM Transactions on Graphics* 37, 4 (2018), 1–12.
- Han Zhang, Ian Goodfellow, Dimitris Metaxas, and Augustus Odena. 2019. Self-attention generative adversarial networks. In *International Conference on Machine Learning*. 7354–7363.

## A REFERENCE MOTION CLIP ACQUISITION

Motion Clip	Collection	File	Start	End
walk		run2_subject1	5758	5791
pace		walk1_subject1	3748	3799
limp		walk1_subject1	4515	4572
swaggering walk		walk2_subject1	2821	2853
sashay walk		walk2_subject1	2613	2645
jaunty walk		walk2_subject1	5002	5044
stomp walk		walk2_subject1	6581	6618
stoop walk		walk4_subject1	986	1014
joyful walk		dance1_subject1	2018	2054
walk with arms akimbo		walk2_subject1	6454	6520
sharp turn during running		run2_subject1	435	479
90-degree turn during walking		walk1_subject1	3386	3448
roll		pushAndStumble1_subject2	4679	4780
fight stance		fightAndSports1_subject4	1096	1110
run	run	run2_subject1	5779	5850
run 2		run2_subject1	5537	5608
spinning jump	spinning and long jump	jumps1_subject1	6682	6772
spinning jump 2		jumps1_subject1	6858	6949
long jump		multipleActions1_subject1	3234	3287
long jump 2		multipleActions1_subject1	3748	3800
get up	get up	fallAndGetUp3_subject1	1318	1404
get up 2		fallAndGetUp3_subject1	2016	2100
get up 3		fallAndGetUp3_subject1	2247	2326
get up 4		fallAndGetUp3_subject1	2473	2580
get up 5		fallAndGetUp3_subject1	2717	2772
punch	punch	fightAndSports1_subject4	1243	1295
punch 2		fightAndSports1_subject4	1109	1148
punch 3		fightAndSports1_subject4	1317	1369
kick	kick	fightAndSports1_subject4	1394	1464
kick 2		fightAndSports1_subject4	971	1036
kick 3		fightAndSports1_subject4	1037	1099
kick 4		fightAndSports1_subject4	1493	1549

Table 5. Reference motion clips acquired from the LAFAN1 dataset. Start and end denote the start and end frame, respectively, of the corresponding file in the LAFAN1 dataset from which a reference motion clip is obtained.

## B POLICY SWITCH SUCCESS RATE VERSUS DISCRIMINATOR SCORE

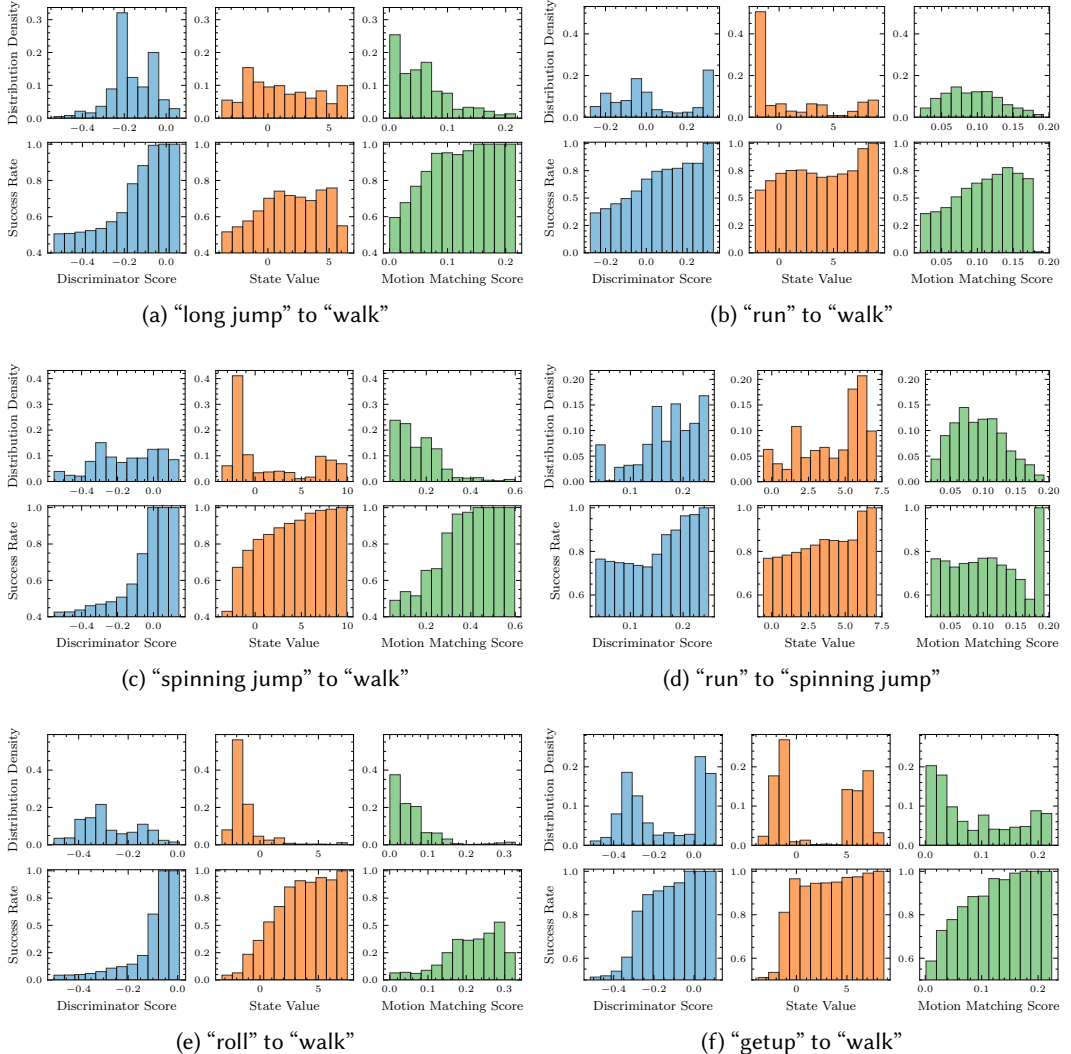


Fig. 14. Distributions of different metrics used for policy switch check (top), and the corresponding success rate with different values used as the switch threshold value (bottom). See Section 6.5 for details of the experiment.